Short Papers

Spatial Optical Beam-Forming Network for Receiving-Mode Multibeam Array Antenna—Proposal and Experiment

Osamu Shibata, Keizo Inagaki, Yoshio Karasawa, and Yoshihiko Mizuguchi

***Abstract*—This paper proposes an array antenna for multibeam reception with a beam-forming network (BFN) that uses spatial optical signal processing and also presents experimental results. In this antenna, signals received at individual antenna elements are converted to optical signals, and are optically divided from the directions of signal arrival by means of optical spatial Fourier transformation, and then the optical signals are reconverted into microwave signals at the BFN. In this BFN, to maintain optical path-length conditions, an optical integrated circuit is employed. We have experimentally investigated the optical signal processing performances of the BFN for multibeam reception. The experimental results show that optical beam direction is changed according to the signal arrival direction of an array antenna. Two multiple RF signals with different phase distributions are separated. The sidelobe level of the optical signal is reduced when amplitude distributions of optical signals are Chebyshev distributions. We also present the signal transmission behavior of this BFN. The measured carrier-to-noise-ratio degradation of this BFN is 2 dB at $\mathrm{BER} = 10^{-6}$ when 118.125-Mb/s QPSK modulated signal is input into the BFN.**

***Index Terms*—Beam-forming network, microwave photonics, multibeam receiving antenna, optical spatial signal processing.**

I. Introduction

An array antenna for multibeam reception requires a beam-forming network (BFN) to separate signals according to the signal arrival directions. Several types of BFN have been proposed such as a microwave-domain BFN, e.g., Butler matrix [1], and a digital beam-forming (DBF) antenna.

Spatial optical signal processing is a BFN technique that uses optical spatial Fourier transformation [3]–[5]. It has a number of advantages in terms of bandwidth, circuit complexity, size, and weight, and processing speed over conventional techniques that use microwave BFN or DBF antennas. With these array antennas, for example, the BFN becomes smaller and lighter and can be controlled at high speed, and the BFN generates less electromagnetic interference, which can affect other electronic devices. In addition, the BFN can be used at any frequency simply by changing the array antenna, giving it excellent broad-band characteristics.

ATR Adaptive Communications Research Laboratories, Kyoto, Japan, has proposed a beam-shaping, beam-scanning, and multibeam transmitting array antenna that uses spatial optical signal processing in its BFN [6]–[8]. However, only a few papers discuss the receive mode of the optical processing array antenna [3]. This is because, as the wavelength of the optical signal is very short, the optical path length is easily disturbed by change in the temperature of the surroundings or a strain condition. The disturbance of the optical path-length condition causes optical phase fluctuation. Therefore, it is difficult to maintain the relative phase differences among the antenna elements in the optical domain. In addition, it is also difficult to maintain the dynamic range of the received signal because there are great losses at an optical modulator even though the power of the signal received by antenna elements is very low. Furthermore, in the case of a receiving mode array antenna, many optical modulators are required, i.e., the number of optical modulators is the same as that of antenna elements; the system becomes relatively complicated and the cost becomes higher than for a transmitting mode array antenna using spatial optical signal processing in its BFN.

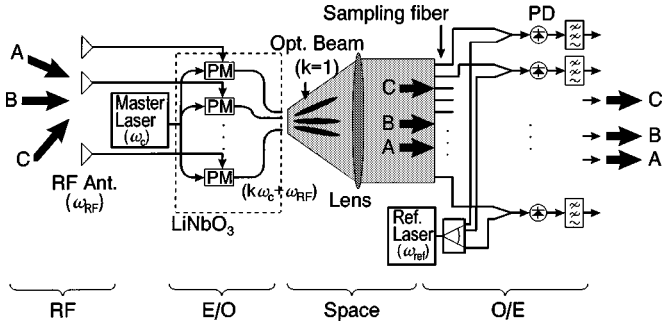

Fig. 1. Schematic view of a spatial optical signal-processing array antenna.

In this paper, we propose a spatial optical signal-processing BFN for a receiving mode multibeam array antenna [9], [10] and present experimental results for basic characteristics. In order to maintain the optical path-length conditions, we employ an optical integrated circuit. This approach avoids complicating the system and reduces the cost. We present experimental results for optical radiation patterns of the BFN when signal arrival direction of a receiving antenna is changed, when two multiple RF signals with different phase distributions are input into the BFN, and when amplitude distributions of optical signals are Chebyshev distributions. We also present the signal-processing behavior of this BFN when a QPSK modulated RF signal is input into the BFN.

II. Antenna Configuration

Fig. 1 shows the basic configuration of the proposed spatial optical signal-processing array antenna for multibeam reception. This antenna consists of four parts. The RF part consists of the RF antenna. The electric-to-optical (E/O) conversion part consists of a master laser and an optical integrated circuit comprises an optical phase modulator (PM) array. The master laser generates an optical source. At the optical PM, the optical source is modulated by the RF signals, i.e., antenna receiving signals are converted from microwave to optical frequency. The signal-processing part radiates all optical signals into space. The lens in Fig. 1 changes the optical beam direction from the radial direction to the parallel direction. It is not an essential component, but if it is not used, the sampling fiber in this figure has to be located on the circumference. The optical-to-electric (O/E) conversion part consists of a reference laser, optical coupler, sampling fiber, and photodiodes (PDs),

Manuscript received October 25, 2000; revised August 9, 2001.

O. Shibata is with the Mobile Communication Laboratory, Corporate Research and Development Center, Toshiba Corporation, Kawasaki 212-8582, Japan (e-mail: osamu.shibata@toshiba.co.jp).

K. Inagaki is with ATR Adaptive Communications Research Laboratories, Kyoto 619-0288, Japan.

Y. Karasawa is with the Department of Electronic Engineering, The University of Electro-Communications, Tokyo 182-8585, Japan.

Y. Mizuguchi is with KDDI Research Laboratories Inc., Saitama 356-8502, Japan.

Publisher Item Identifier S 0018-9480(02)04046-2.

which reconvert the optical signals into RF or IF signals. The reference laser is phase locked to the master laser. All radiated optical beams are sampled by the sampling fiber, coupled with the optical signal of the reference laser, and reconverted to RF or IF signals at the PD.

When an RF signal arrives at the RF antenna from a particular direction, the array antenna has a certain phase distribution. Each antenna received RF signal is input into each PM. The PM formula is as follows:

$$f(t) = A_0 \cos\left\{\omega_c t + m\cos(\omega_{\rm RF} t + \phi)\right\} = A_0 \sum_{k=-\infty}^{\infty} J_k(m) \cos\left\{(\omega_c + k\omega_{\rm RF})t + k\left(\phi + \frac{\pi}{2}\right)\right\} \quad (1)$$

where ω_c is the frequency of the master laser, $\omega_{\rm RF}$ is the RF frequency, and ϕ is the RF phase. When we focus on the first upper sideband (1st USB) component of the modulated optical signal $(k = 1)$, the formula is written as

$$f(t)_{k=1} = A_0 J_1(m) \cos\left\{(\omega_c + \omega_{\rm RF})t + \left(\phi + \frac{\pi}{2}\right)\right\}. \quad (2)$$

This formula shows that the phase distribution of the 1st USB component of the modulated signal is of the same value as the input RF signal phase distribution; i.e., the phase distribution of the optical path is the same value as the phase distribution of the array antenna. When these modulated optical signals are radiated into space, the optical beam is tilted according to the phase distribution determined by the antenna receiving signal arrival direction. The radiation pattern of the optical signal is calculated by an array antenna formula [11]. The radiation pattern of the optical beam is determined by the phase and amplitude distributions of the optical signal; therefore, maintenance of the optical phase stability constitutes an important problem. It is very difficult to achieve the optical phase stability because the optical path length is easily disturbed by change in the temperature of the surroundings or a strain condition. To maintain the optical path-length conditions, we integrate optical waveguides and optical PMs on an $LiNbO_3$ substrate. Integration of the optical waveguides on an $LiNbO_3$ substrate means that the optical waveguides are disturbed by the same conditions; therefore, the relative optical path-length conditions are preserved.

When the plural signals arrive at the RF antenna, the signals are separated into the beam arrival directions through the spatial optical signal processing. Fig. 1 shows that, when three RF signals arrive at the antennas from different directions, three optical beams are radiated from the edge of the substrate to different directions. These optical beams are then sampled by the sampling fiber and reconverted to RF or IF signals at the O/E part. Though the radiated optical signal comprises many components of different frequency, these components are reconverted to the different frequencies when the master laser is phase locked to the reference laser with particular frequency offset. Therefore, only the 1st USB component can be obtained by using RF or IF filters.

III. Experimental Investigation

A. Optical PM Array

To verify our proposal, we fabricated the optical PM array shown in Fig. 2 and measured the basic characteristics. Fig. 3 shows the schematic view of the fabricated optical PM array. The eight optical PMs and seven variable power dividers (VPDs) are integrated on a z-cut $LiNbO_3$ substrate. We use Ti-indiffused single-mode optical waveguides at 1.3-μm wavelength band. The VPDs have reverse $\Delta\beta$-type electrodes [12] for changing the division ratio of the optical signal according to the applied voltage on the electrodes.

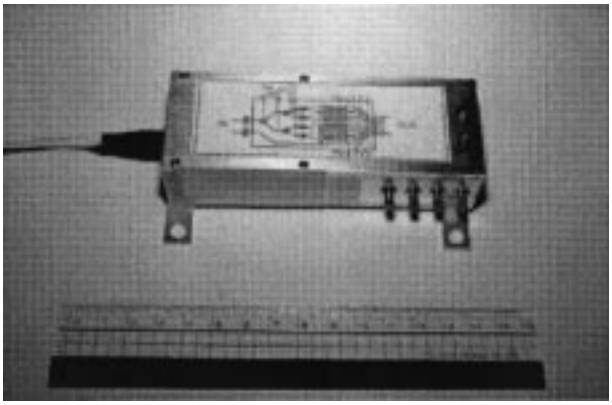

Fig. 2. Fabricated eight-element optical PM array. Scale length in this photograph is 16 cm.

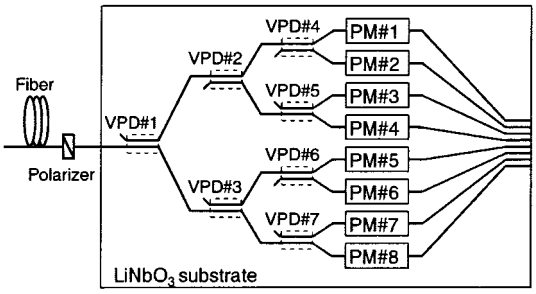

Fig. 3. Schematic view of fabricated eight-element optical PM array.

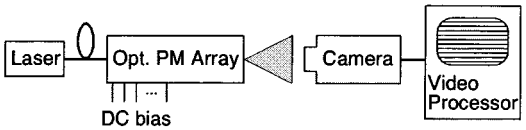

Fig. 4. Experimental setup to measure V_π value.

TABLE I
V_π Value of Optical PM

Phase Modulator	V_π
PM #1	5.4 V
PM #2	5.2 V
PM #3	5.2 V
PM #4	5.2 V
PM #5	5.2 V
PM #6	5.3 V
PM #7	5.2 V
PM #8	5.2 V

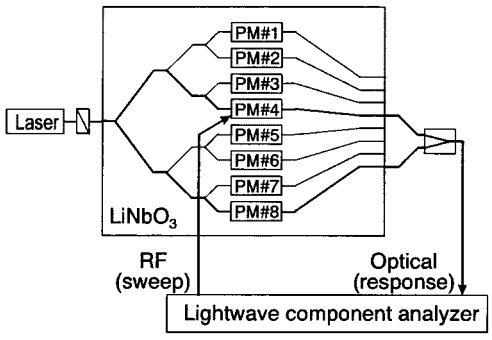

Fig. 5. Experimental setup to measure frequency responses when the measured optical PM is PM#4.

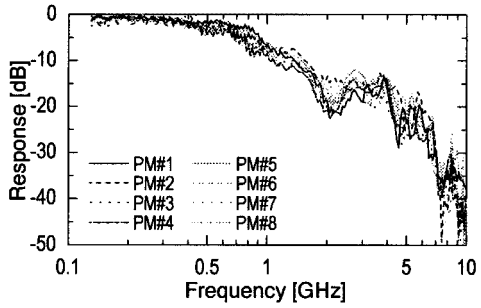

Fig. 6. Frequency responses of optical PMs.

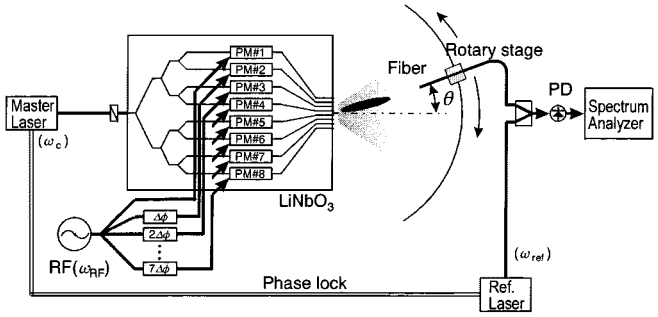

Fig. 7. Experimental setup to measure the optical radiation pattern.

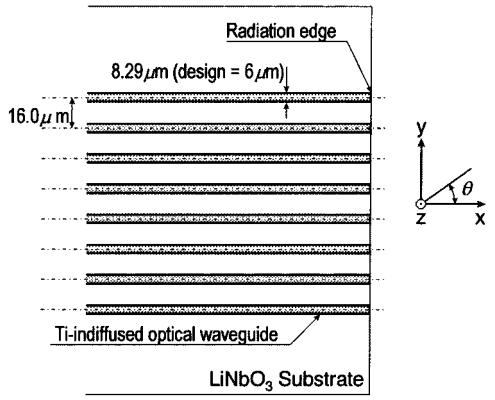

Fig. 8. Edge structure of fabricated $LiNbO_3$ substrate where optical beams radiate into space.

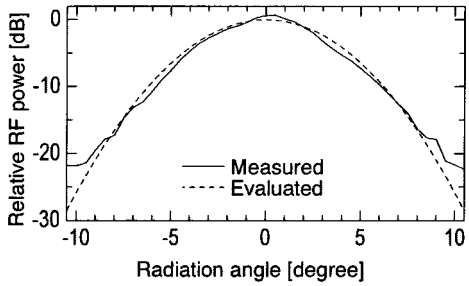

Fig. 9. Single-element radiation pattern in the BFN when the RF signal was input into PM#4.

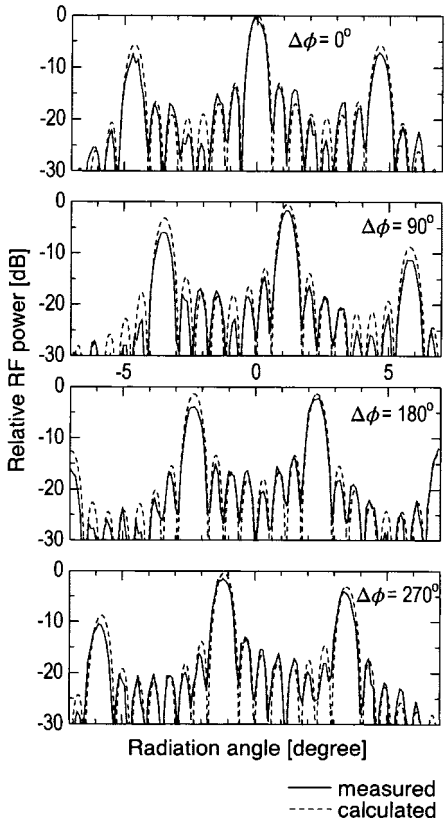

Fig. 10. Radiation patterns of fabricated optical PM array.

First, we measured V_π of the PM. Here, V_π is the dc voltage of an optical wave phase shift of 180° in the PM, when the PM works as a phase shifter. If V_π is a small value, a large phase shift can be obtained by a small RF signal. In order to obtain a highly efficient E/O converter, a PM with a small V_π is required.

The experimental setup is shown in Fig. 4. When the measured optical PM was PM#4, the VPDs were set to distribute the optical signal to PM#4 and PM#5, and radiated optical beams were observed with the camera. We examined the periodic motion of the optical radiation pattern at the time the applied dc voltage of PM#4 increased. The V_π values of other PMs are measured by a similar procedure. Table I presents the obtained V_π values. These results show that the obtained V_π values are of almost equal characteristics.

At the optical PM in this BFN, the optical signal was modulated by the antenna-received RF signal; therefore, the performance of the optical PM at high frequency is important. Thus, we measured the frequency responses of the PM using an HP 8703A lightwave component analyzer. The experimental setup is shown in Fig. 5. In this experiment, the optical PM was set in the Mach–Zehnder interferometer path. When it is set in the Mach–Zehnder interferometer path, it works as an intensity modulator (IM). To obtain sufficient dynamic range in the measurement, we used another optical PM array with the same optical PM structure, but where the output optical signals were incident to the optical fibers. The optical beam from the laser was input into the fiber-coupled optical PM array. When the measured optical PM was PM#4, the VPDs were set to distribute the optical signal to PM#4 and PM#8. The optical coupler coupled the output optical signals of these optical PMs. The swept RF signal was input into the optical PM and we measured the optical intensity response of the output signal of the optical coupler. The frequency responses of other PMs are measured by a similar procedure. Fig. 6 shows the obtained frequency responses. This figure indicates that the frequency of the optical response dropped -3 dB at approximately 450 MHz; i.e., the optical PMs worked in the low-frequency region below 450 MHz. Since the aim of our experiment is to investigate the basic characteristics, it is sufficient to experiment in the low-frequency region. Note that high-frequency characteristics will improve if a traveling-wave-type PM is used [13].

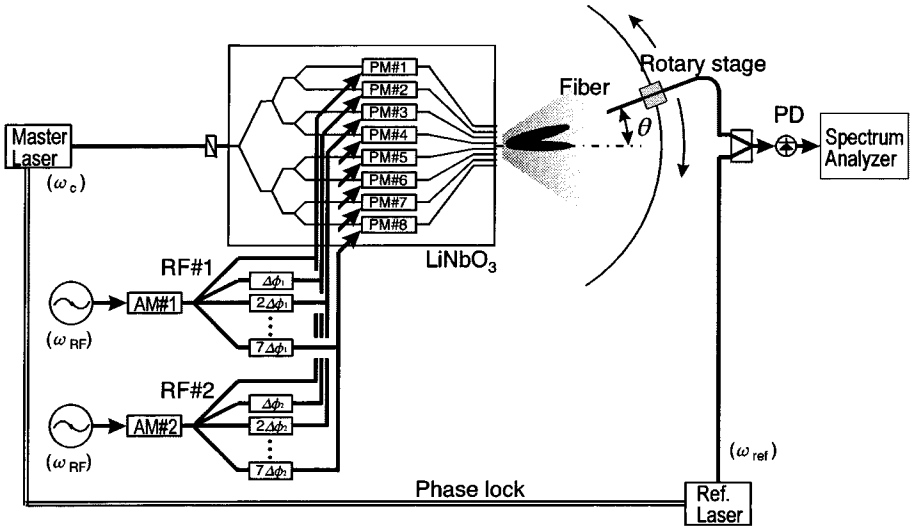

Fig. 11. Experimental setup to measure the optical radiation pattern when two RF signals are input into BFN.

B. Optical Radiation Patterns of BFN

1) Experimental Setup: To investigate the optical signal-processing behavior, we measured the radiation pattern of the 1st USB component of the optical signal in the BFN. Instead of an actual antenna receiving RF signal, we used a signal generator and phase shifters to investigate the basic characteristics of the BFN. Fig. 7 shows the experimental setup. The phase difference $\Delta\phi$ was changed by the phase shifters to simulate the antenna-received signal when an RF signal arrival direction was changed. The lasers were Nd : YAG lasers at 1.319-μm-wavelength band and had exceptionally high-frequency stability. We phase locked the master laser to the reference laser with individual frequency offset to produce the 1st USB and other frequency components with different microwave frequencies. In this experiment, the lasers were phase locked at 400 MHz and the output power of the master laser was 5 mW. The RF signal frequency was 300 MHz and the amplitude at the input port of the optical PM was 0 dBm. Radiated optical beams were sampled by a fiber, combined into an optical signal from the reference laser, and detected by a PD. We rotated the fiber on the rotary stage and measured the 1st USB component of the detected signal at 100 MHz by a spectrum analyzer to obtain the radiation pattern. The distance from the edge of the $LiNbO_3$ substrate to the fiber was 22 mm, which satisfied the far-field condition.

2) Element Pattern: The radiation pattern of an array antenna is calculated by using the element factor and array factor [11]. The element factor is the radiation pattern of one element. It is determined by the optical waveguide width of the radiating edge. Fig. 8 shows the radiating edge of the fabricated $LiNbO_3$ substrate. The optical waveguides were Ti-indiffused waveguides with a designed width of 6 μm and an element spacing of 16 μm. Considering the diffusing process, there are some differences between the fabricated width and designed width of the waveguide. To evaluate the element factor, we measured the optical radiation pattern of the BFN when the RF signal was input into only one PM.

The solid line in Fig. 9 shows the obtained radiation pattern. The horizontal axis indicates the angle from the center, and the vertical axis indicates the relative microwave signal amplitude detected by the PD, which is equal to the value of the relative power of the 1st USB component of the optical signal. The 3-dB beamwidth of the obtained radiation pattern is approximately 5°. The broken line indicates the Gaussian beam whose mode field radius at the edge of the optical waveguide is 8.29 μm. This value is 2.29 μm wider than the designed width. Considering the Ti-indiffused waveguide, the obtained value accords with expectations. We can then obtain the element factor. The array factor of the linear array is determined by the element spacing normalized by the optical wavelength, amplitude, and phase distributions. We then obtain all parameters to calculate the radiation patterns.

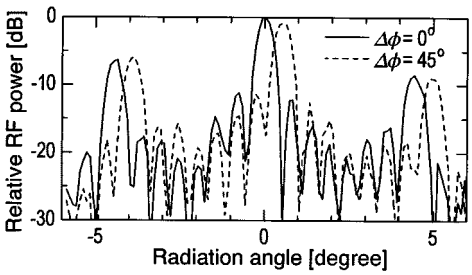

Fig. 12. Radiation pattern of optical PM array with two different RF signals input to the BFN.

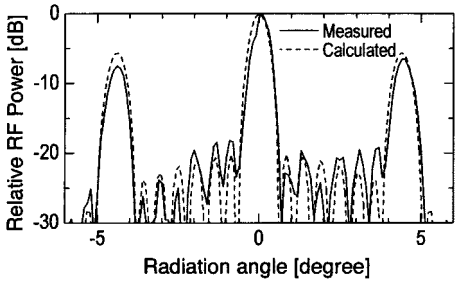

Fig. 13. Radiation pattern of optical PM array when the optical distributions are Chebyshev distributions with sidelobe level design of less than −20 dB.

3) Main Beam Scanning: Next, we measured the radiation patterns of the BFN when the signal arrival direction was changed. The VPDs were set to distribute optical beams to the eight optical PMs with uniform amplitude distributions.

Fig. 10 shows the obtained radiation pattern. The value of $\Delta\phi$ indicates the phase difference between adjacent RF signals; when it was 0°, the signal arrived from the center. The values of $\Delta\phi$ of 90°, 180°, and 270° corresponded to the signal arrival directions of 60°, ±90°, and

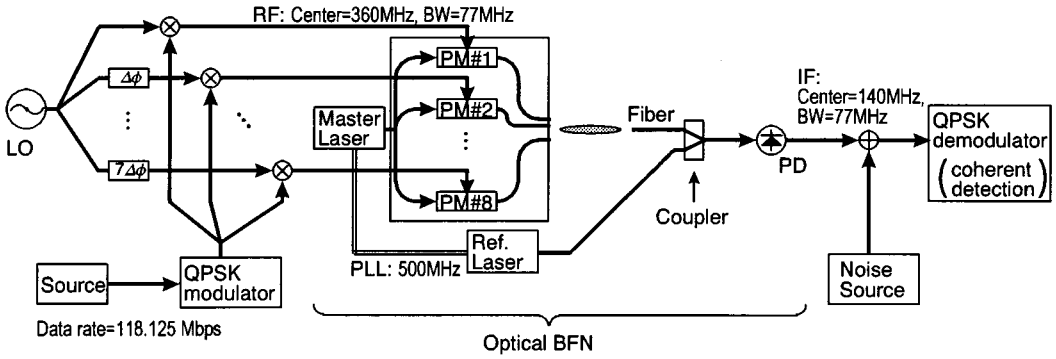

Fig. 14. Experimental setup to investigate the characteristics when a QPSK modulated signal is input.

-60° tilted from the center, respectively, when the RF antenna element spacing was a half-wavelength.

The obtained radiation pattern was in good agreement with the calculated value and the beam tilted when the signal arrival direction was changed. The grating lobes appeared at approximately 4.8° intervals. It appears as the same principle of the well-known physical phenomenon of the interference fringes. This is because optical waveguide spacing of the radiating edge is larger than the optical wavelength. Although the grating lobes appeared, only the main lobe is required for spatial signal processing. Therefore, if we fabricated the BFN to acquire the main lobe, signal processing can be done. Since the grating lobes were unnecessary for signal processing, there are unused signal powers of signal processing. That is to say, a high grating lobe means large signal loss of the BFN. Therefore, we have been studying to develop a spatial optical BFN with less optical leakage for the direction of grating lobe appearance.

4) Multiple Signal Processing: In this BFN, when a number of sampling fibers were arranged side by side, multiple signals were separated in the optical domain without system modification. In this experiment, we investigated the multiple signal-processing behavior of the RF signals, when two different phase distributions are combined and input into the BFN. Fig. 11 shows the experimental setup. The RF signals were of the same frequency, i.e., 300 MHz. To distinguish between the two signals, the signals were amplitude modulated (AM) at a different frequency and the amplitude of the AM signal component was measured at the detected frequency. The phase differences of $\Delta\phi$ were 0° and 45° where signal arrival directions were at the center and 15° tilted from the center when the simulated antenna element spacing was a half-wavelength. In this case, the crossover level of the main beams is approximately -3 dB.

Fig. 12 shows the obtained radiation patterns. The patterns are in good agreement with the calculated values, and these signals are separated into different angles. When the sampling fibers are located at the center and 0.58° from the center, the signals will be detected independently. When an array antenna with more elements is used, the 3-dB beamwidth will be narrowed and the minimum signal separation angle will be obtained.

Though the grating lobe appeared at intervals of approximately 4.8° in front of the waveguide, as shown in this figure, only the main lobe is required for spatial signal processing. Therefore, if the optical beams are sampled within $\pm 2.4^\circ$ region, these signals can be obtained.

5) Chebyshev Distributions: Next, we set the VPDs to change the optical signal power distributions by changing the VPD on the $LiNbO_3$ substrate. Fig. 13 shows the obtained radiation pattern when the optical power distribution was a Chebyshev distribution [11] with a sidelobe level design of less than -20 dB. The sidelobe levels clearly decline compared with the equal optical distributions shown in Fig. 10. The peak level of the sidelobe is -17 dB, which is 3 dB greater than the design level. This is mainly due to optical distributions that are incorrect for the exact design distributions.

In this structure, the level of signal leakage at different angles can be reduced compared with those of uniform optical distributions instead of increasing beamwidth. This result confirms that the array antenna weight distributions can be changed by changing only the optical signal power distributions.

TABLE II
PARAMETERS OF QPSK MODULATOR AND DEMODULATOR

Data rate	118.125 Mbps
Roll-off filter	root cosine roll-off roll-off factor = 0.3
Center frequency	140 MHz
Occupied bandwidth	77 MHz
Detection method	coherent detection

C. Characteristics When a QPSK Modulated Signal is Input

The optical signal frequency in this experiment was 227 THz; therefore the broad-band signal at the microwave frequency domain could be regarded as a narrow-bandwidth signal at the optical domain. To investigate the wide-band signal-processing behavior, a 118.125-Mb/s QPSK modulated signal with an occupied bandwidth of 77 MHz was employed to evaluate the wide-bandwidth operation. The experimental setup is shown in Fig. 14. The parameters of this experiment are listed in Table II. The center frequency of the input signal to the BFN was 360 MHz and the power was 0 dBm. The relative bandwidth of the signal processing was 21%. The lasers were phase locked at 500 MHz. The power of the optical beam of the master laser was 40 mW. The PD output signal was an IF signal with a center frequency of 140 MHz.

The carrier-to-noise ratio (CNR) obtained by the spectrum analyzer was approximately 20 dB. In this experiment, which is only a fundamental experiment, we can obtain the CNR of 20 dB by using the master laser of 40 mW. If a higher power laser were employed, we would be able to reduce the degradation of the dynamic range and, thus, obtain higher CNR.

Fig. 15 shows the eye pattern of the modulation signal and that of the demodulated signal. The eye opening is clear. Fig. 16 shows the bit error rate (BER) performance with additive white Gaussian noise at the IF signal. The broken line indicates the performance when the QPSK demodulator was directly connected to the QPSK modulator. The dots and solid line indicate the performance of the whole system.

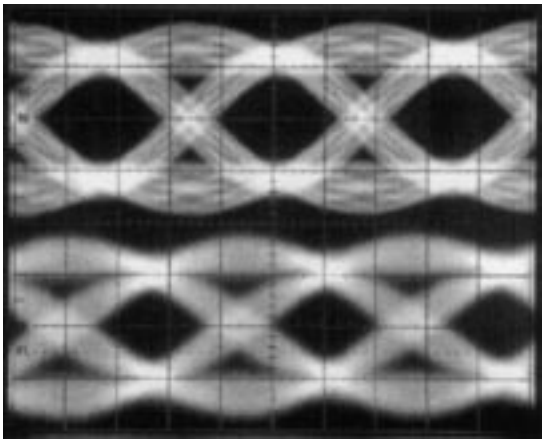

Fig. 15. Eye patterns of baseband QPSK signals. Upper: modulation signal. Lower: demodulated signal under the condition that $\mathrm{CNR} = -20$ dB.

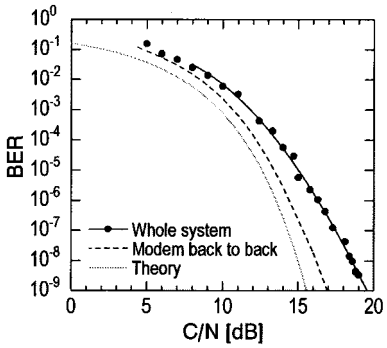

Fig. 16. BER performance of BFN.

The CNR degrades 2 dB at a BER of 1×10^{-6}. This mainly seems to be due to the optical path length being disturbed at the fiber from the master laser to the optical PM array, at the reference laser to the optical coupler, and at the sampling fiber. It will be improved when the BFN is optimized. Another possibility is that it is due to the mutual coupling of the RF frequency at the optical PMs. It will be improved, however, by designing the electrode of the optical PMs so as to decrease the RF mutual coupling.

These results show that the optical signal-processing BFN works with the wide-band signal-processing BFN.

IV. Conclusion

We have proposed a spatial optical signal-processing BFN for a receiving mode multibeam array antenna and presented the basic characteristics of this BFN. With the antenna, received signals are converted to optical signals, and are optically divided from the beam arrival directions by optical spatial Fourier transformation, and then the optical signals are reconverted into microwave signals. To maintain the optical path-length conditions, an optical integrated circuit is employed.

Experimental results have been presented that show that the optical beam is tilted when the signal arrival direction is changed. Two RF signals with different phase distributions are separated. The sidelobe level of the optical signal is decreased when the optical signal distributions are Chebyshev distributions. The CNR degradation is 2 dB at a BER of 10^{-6} when a 118.125-Mb/s QPSK modulated signal is input into this BFN.

One of the main problems concerning this BFN is that optical loss of the BFN causes degradation of the dynamic range of this system and, thus, high CNR cannot be obtained. When a higher power laser is employed, degradation of the dynamic range can be avoided. In our experiment, which is only a fundamental experiment, we obtained the CNR of 20 dB by using the master laser of 40 mW. If a higher power laser were employed, we would be able to obtain higher CNR; our proposed optical BFN is applicable to systems satisfying required BER for practical applications such as satellite communication systems and mobile and personal communication systems.

Using the proposed approach, we can develop a broad-band spatial optical BFN for receiving a mode multibeam array antenna.

Acknowledgment

The authors are grateful to Dr. B. Komiyama, ATR Adaptive Communications Research Laboratories, Kyoto, Japan, for his encouragement. The authors are also indebted to Dr. Y. Ji, formerly of ATR Adaptive Communications Research Laboratories, and T. Inoue, formerly of ATR Adaptive Communications Research Laboratories, for useful discussion.

References

[1] J. Butler and R. Lowe, "Beam-forming matrix simplifies design of electronically scanned antennas," *Electron. Design*, pp. 170–173, Apr. 1961.

[2] R. Miura, T. Tanaka, I. Chiba, A. Horie, and Y. Karasawa, "Beam-forming experiment with a DBF multibeam antenna in a mobile satellite environment," *IEEE Trans. Antennas Propagat.*, vol. 45, pp. 707–714, Apr. 1997.

[3] G. A. Koepf, "Optical processor for phased array antenna beamformation," *Proc. SPIE–Inst. Soc. Opt. Eng.*, vol. 477, pp. 75–81, May 1984.

[4] A. Seeds, "Optical technologies for phased array antennas," *Trans. Inst. Electr. Eng. Jpn. C*, vol. E76-C, no. 2, pp. 198–206, Feb. 1993.

[5] I. Ogawa, K. Hirokawa, T. Kitoh, and H. Ogawa, "Novel multibeam forming network miniaturized by optical slab waveguide," in *Proc. ISAP'96*, vol. 1, pp. 121–124.

[6] Y. Konishi, W. Chujo, and M. Fujise, "Carrier-to noise ratio and sidelobe level in a two-laser model optically controlled array antenna using Fourier optics," *IEEE Trans. Antennas Propagat.*, vol. 40, pp. 1459–1465, Dec. 1992.

[7] K. Yamada, I. Chiba, and Y. Karasawa, "Frequency characteristics of a beamforming network of an optically controlled array antenna and its radiation pattern measurements," *IEICE Trans. Electron.*, vol. E79-C, no. 1, pp. 68–73, Jan. 1996.

[8] Y. Ji, K. Inagaki, R. Miura, and Y. Karasawa, "Optical processor for multibeam microwave array antennas," *Electron. Lett.*, vol. 32, no. 9, pp. 822–824, Apr. 1996.

[9] O. Shibata, K. Inagaki, Y. Ji, and Y. Karasawa, "Spatial optical processing array antenna for multibeam reception," presented at the MWP'96, Paper WE3-4.

[10] ——, "A multibeam receiving array antenna by means of spatial optical signal processing," presented at the IEEE Antennas Propagat. Symp., 1997, Paper 36.4.

[11] W. L. Stutzman and G. A. Thiele, *Antenna Theory and Design*. New York: Wiley, 1981.

[12] H. Kogelnic and R. V. Schmidt, "Switched directional coupler with alternating $\Delta\beta$," *IEEE J. Quantum Electron.*, vol. QE-12, pp. 396–401, July 1976.

[13] K. Noguchi, O. Mitomi, H. Miyazawa, and S. Seki, "A broad-band $Ti:LiNbO_3$ optical modulator with a ridge structure," *J. Lightwave Technol.*, vol. 13, pp. 1164–1168, June 1995.